



Process simulation of chemical looping gasification of biomass using Fe-based oxygen carrier: Effect of coupled parameters

Shuaijie Xue^a, Xudong Wang^{b,c,*}

^a Science and Technology on Liquid Rocket Engine Laboratory, Xi'an Aerospace Propulsion Institute, 710100, Xi'an, China

^b School of Mechanical and Power Engineering, Nanjing Tech University, Nanjing, 211816, China

^c Key Laboratory of Energy Thermal Conversion and Control of Ministry of Education, School of Energy and Environment, Southeast University, Nanjing, 210096, China

ARTICLE INFO

Handling editor: Kathleen Aviso

Keywords:

Biomass

Chemical looping gasification

Process simulation

Coupled parameters

ABSTRACT

Chemical looping gasification (CLG) of biomass is an efficient way to obtain high-quality syngas without the need of air separation. It offers a carbon-negative and clean way for the utilization of biomass while syngas is used combining with carbon capture. A simulation model of CLG process with continuous feedstock of pine sawdust is constructed and investigated in this work. The iron-based oxygen carrier (OC) is adopted to offer lattice oxygen. This model is validated using the experimental results from literature to demonstrate its feasibility for CLG of biomass. Then, the operating parameters of gasification temperature, amounts of steam and OC are changed to investigate their effects on the gasification performances. Results demonstrated that increasing the temperature, OC and steam flow is beneficial to intensify the carbon conversion efficiency. When the gasification temperature is 880 °C, carbon conversion efficiency and gasification efficiency reach 92.76% and 81.87%. The carbon conversion efficiency rises from 76.81% to 82.18% when OC mass flow is changed from 0 to 1.5 kg/h. Coupled effects of the amounts of reaction temperature, OC mass flow and steam molar flow are also investigated while two of them are changed simultaneously. The minimum and maximum values of gasification efficiencies are 62.13% and 77.73% when the amounts of steam and OC are (0 mol/h, 1.0 kg/h) and (1.0 mol/h, 0 kg/h), respectively. When both of them increases to 1.0 kg/h or 1.0 mol/h, the carbon conversion efficiency reaches the maximum value of 88.57%. The coupled effects of temperature and OC or steam amount demonstrate that the carbon conversion efficiency is mainly determined by temperature at lower-temperature range. Though both of OC and steam can offer oxygen in CLG, due to the different oxidation ability, their effects on gasification efficiency are opposite. Investigation on coupled effects of multiple parameters offers thorough information for the system performance evaluation, which can be used for further system optimization.

1. Introduction

Chemical looping technologies have been concentrated due to its properties of high efficiency, low cost for carbon separation or air separation, etc. The chemical looping concept is based on two separated redox processes of a kind of carrier medium, which is called oxygen carrier (Adánez et al., 2018). The investigation on chemical looping is always related to the oxygen carrier (Yu et al., 2019), fuel (Adánez et al., 2018; Lin et al., 2020a), and reactor (Lin et al., 2020a). These processes take place in two reactors where the oxygen carrier is reduced and oxidized. There are different chemical looping technologies according to the objectives, such as chemical looping combustion of black liquor (Man et al., 2020), coal (Wang et al., 2018a) and solid waste (Wang

et al., 2021), chemical looping gasification (Detchusananard et al., 2020; Udomsirichakorn and Salam, 2014), chemical looping air separation using Cu- (Deng et al., 2018) or Mn-based oxygen carrier (Cao et al., 2019), chemical looping reforming using steam (Stenberg et al., 2018) and dry reforming using CO₂ (Huang et al., 2016a), chemical looping ammonia production assisted by plasma (Sarafranz and Christo, 2021) or renewable energy (Weng et al., 2021) and so on.

Biomass is a kind of renewable resource and chemical looping gasification (CLG) of biomass has been demonstrated to be an efficient way to obtain high-quality syngas without the need of air separation, which is a cleaner disposal way comparing with traditional gasification. During biomass chemical looping gasification (BCLG) process, biomass is gasified in gasifier (GR) where the gasification agent and oxygen carrier (OC) are introduced into. Reduced OC is demonstrated to be a catalyst

* Corresponding author. School of Mechanical and Power Engineering, Nanjing Tech University, Nanjing, 211816, China.

E-mail address: xdwang_seu@seu.edu.cn (X. Wang).

<https://doi.org/10.1016/j.jclepro.2022.131839>

Received 9 October 2021; Received in revised form 15 April 2022; Accepted 15 April 2022

Available online 20 April 2022

0959-6526/© 2022 Elsevier Ltd. All rights reserved.

Nomenclature

C	gas composition
E_A , ΔH	activation energy
G_V	total gas yield
k , K	kinetic constant
k_o , K_o	pre-exponential factor
m	mass feeding rate
n	gas molar flow
p	partial pressure
r	reaction rate
r_g	grain radius
ROC	oxygen transport capacity
T	temperature
X	conversion

Greek symbols

ρ_m	molar density
η	gasification efficiency
η_c	carbon conversion efficiency

Abbreviations

AR	air reactor
BCLG	biomass chemical looping gasification
CFD	computational fluid dynamic
CLG	chemical looping gasification
GR	gasifier
LHV	Lower heating value
OC	Oxygen carrier

for biomass tar cracking (Hu et al., 2020). The reduced OC is then separated and oxidized in another reactor, namely air reactor (AR). The gasification products of CLG are always of high content of combustible gases and they are not diluted by N_2 in air (Huang et al., 2016b). Many kinds of biomass have been investigated on their CLG in fixed bed, fluidized bed and circulating fluidized bed (Lin et al., 2020a; Mohamed et al., 2020). Typical ones include pine, rice husk, rice straw, peanut shell, wheat straw and so on. As iron-based OC is low-cost and environmentally friendly, it has been widely used in chemical looping technologies, such as iron ore in pilot-scale unit (Wang et al., 2020a), iron ore in fixed reactor (Wang et al., 2020b), hematite (Wei et al., 2018) and lean iron ore (Wang et al., 2018b). Hu et al. compared the BCLG performances of wheat straw using iron-based OCs which are Fe_2O_3 supported by Al_2O_3 , TiO_2 , SiO_2 and ZrO_2 . Results revealed that 60% Fe_2O_3 on Al_2O_3 has the highest performance in gas yield and carbon conversion (Hu et al., 2018). Further, this OC was used to gasify rice straw, corn stalk, peanut shell and wheat straw for BCLG (Hu et al., 2019). The kinetics of corn straw CLG with Fe-based OC was studied in thermogravimetric analyzer by Yan et al. (2020). Biomass char was used as fuel in fixed-bed reactor with natural iron ore as OC. The CLG experiment was carried out under both inert atmosphere and steam. The addition of steam in gasification agent greatly improved the carbon conversion and gas yield (Huang et al., 2016b). In addition, interconnected fluidized bed system was employed to evaluate the circulation performances. Rice husk CLG in a 25 kW interconnected fluidized bed had higher carbon conversion efficiency and gas yield with the hematite as OC at 860 °C, which was recognized as the optimal gasification temperature (Ge et al., 2016). In a 1.5 kW interconnected fluidized beds system, synthetic Fe-based OC is used for the CLG of pine wood. The autothermal condition was experimentally obtained, under which the gas efficiency reached 68% (Samprón et al., 2020). In the same unit, Condori et al. adopted ilmenite as OC to investigate the BCLG performances of pine wood (Condori et al., 2021). The lattice oxygen in gasification process was controlled by changing the air into air. The CLG of pine sawdust was conducted in 10 kW interconnected circulating fluidized beds using synthetic Fe_2O_3 OC. The operating results showed the optimal feeding rate of biomass should be 2.24 kg/h in this apparatus (Wei et al., 2015). The CLG of pine sawdust with iron ore in a dual fluidized bed gasifier showed that the optimal gasification temperature was 820 °C while the mass ratio of steam to feedstock was 1.5 (Zeng et al., 2015). In order to promote the biomass gasification, bimetallic OCs were prepared and applied to BCLG. He et al. found that a small amount of CuO into Fe-based OC could potentially improve the solid conversion in CLG due to its oxygen uncoupling property (He et al., 2013). Xue et al. investigated the CO selectivity in biomass char CLG using different OCs of Fe_2O_3 , Fe_2O_3/CaO and $CaFe_2O_4$ (Xue et al., 2019). The $CaFe_2O_4$ was found to be the best in CO selectivity. Huang et al.

analyzed the thermodynamic and kinetic performances of biomass char CLG using $NiFe_2O_4$ as OC (Huang et al., 2017). The ratio of OC to biomass char as 0.3 was found to reach the highest gasification efficiency. Zheng et al. conducted the CLG experiment using torrefied eucalyptus as fuel in TG-MS and Py-GC/MS. $NiFe_2O_4$ was employed as OC (Zheng et al., 2020). The optimal torrefaction temperature and mass ratio of OC to feedstock were found to be 280 °C and 1.25, respectively. Using $NiFe_2O_4$ as OC in BCLG, an optimal ratio of lattice oxygen to biomass was found to be 0.51 at 850 °C while steam of CO_2 was added into carrying gas. The absence of steam or CO_2 could promote the conversion of biomass (He et al., 2019). The kinetic analysis of pine with $NiFe_2O_4$ OC in BCLG was also studied (Lin et al., 2020b).

Despite of the fact that experimental works can reveal the BCLG performances practically, it is hard to show the detailed evolution process in reactor system spatiotemporally. Simulation is an available tool for this purpose. Computational fluid dynamic (CFD) offers detailed information about the gas-solid distribution and evolution in a reactor, which can also be used for pre-validation or design of a single reactor (Wang et al., 2021a) or a reactor system (Wang et al., 2020c). Some CFD works have been conducted on BCLG using one-dimensional (Li et al., 2019a) or two-dimensional method (Li et al., 2019b). Interestingly, researchers developed a 1.5-dimensional simulation software named CeSFaMB, and they conducted the chemical looping simulations using CuO (Zylka et al., 2019) and ilmenite (Zylka et al., 2020) as oxygen carrier. Another important simulation is the process modelling, which can be used to evaluate the thermodynamics (Wang et al., 2021b) and techno-economic feasibility of a system (Sun and Aziz, 2021). Li et al. designed a CLG process for butanol production using lignocellulosic biomass. The economic assessment was conducted based on process modelling (Li et al., 2020). A simulation process of BCLG combined cycle was established for power production (Mohamed et al., 2020). The technical and economic evaluations of this cycle were performed with or without carbon capture and storage, demonstrating the potential and feasibility of BCLG. Gopaul et al. compared two CLG processes using poultry litter as fuel (Gopaul et al., 2014). The optimal operating conditions were determined according to the simulation results of Aspen plus. Using the mixture of indium oxide and indium slurry as OC, Sarafraz et al. investigated the techno-economic feasibility of a BCLG system (Sarafraz and Christo, 2020). The BCLG of pine wood using Fe-based OC was simulated to determine the autothermal conditions (Samprón et al., 2021). The heat and mass balances were analyzed and different oxygen control methods were adopted to maximize the gas production. There are also some other works focusing on chemical looping gasification using black liquor (Darmawan et al., 2018) or microalgae (Nurdiawati et al., 2019) as feedstock.

As the detailed reaction models can offer reliable information in reactor while process model can be used to assess the techno-economic

analysis, the combination of detailed reaction model and process model can be important for system scale-up. Few works on the combination of them have been reported in the field of BCLG. The CFD simulation is always used to investigate the internal flow and reaction behavior, which offers information for the optimization of the structure and operating parameters. In this work, we employed the process simulation to theoretically analyze the effect of operating parameters on the CLG performance. Comparing with CFD simulation, this method is quite suitable for the study of effects of multiple variables. In this work, a detailed CLG process model of pine sawdust is established with reaction kinetic models while Fe_2O_3 is used as OC. This kinetic model was validated using experimental data, showing a satisfactory feasibility. In addition, though in many current literatures, the effects of multiple parameters were studied. In each case, only one parameter was changed. That is not enough for a clear understanding of the chemical looping gasification system, because one parameter might have slight effect on gasification performance while others are fixed in specific range. When the range of others parameters are changed, the effect of that parameter might change a lot. Thereof, the investigation of coupled effects of these parameters is important and necessary. In this work, different operating parameters are changed to assess the total gas yield, carbon conversion efficiency and gasification efficiency while steam is added into the gasification agent. Coupled effects of the temperature, amounts of OC and steam are also evaluated. The CLG performances are affected by multiple parameters and their significances are different in variable conditions. Results offer reliable information for the future design and operation optimization of CLG system.

2. Biomass CLG process models

2.1. Process model

In previous work, Huang et al. investigated the experimental results of CLG of pine sawdust (Huang et al., 2013). A laboratory fluidized bed is adopted as the gasifier. Once the biomass was added into the reactor, it went through fast devolatilization and pyrolysis, then the char was gasified while tar was cracked. In CLG, Fe_2O_3 was adopted as the OC for combustible gas production. In a general CLG process, there are air reactor (AR) and fuel reactor. In fuel reactor, the solid feedstock is gasified by oxygen carrier with the assistant of gasification agent, where the oxygen carrier is reduced. In air reactor, the reduced oxygen carrier reacts with air and it is regenerated, which is quite fast. On the contrary, the reactions of char gasification and oxygen carrier reduction are of

relatively low rates. That means the rate control reaction in chemical looping technology always takes place in fuel reactor. Also, reactions in fuel reactor are complex. Thereof, this work also focuses on the performance of fuel reactor in chemical looping gasification of biomass. To simulate this complex process, a simulation model is established as Fig. 1.

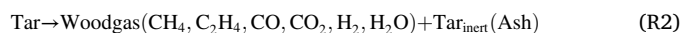
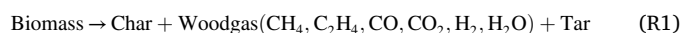
A two-step pyrolysis model of biomass consists devolatilization and tar cracking. In first pyrolysis reactor, biomass is decomposed to biomass char, woodgas and tar while tar is further cracked into gaseous products in second step. All products except ash are mixed and introduced into a gasifier (GR) while OC and gasification agent are also introduced into GR. Herein, the char gasification and CLG take place. After gasification, the gases are separated from reduced OC and then are condensed for gasification products, namely combustible gas.

The biomass used in this work is pine sawdust, which is same as that in Ref (Huang et al., 2013). The ultimate and proximate analyses of this kind of biomass are listed in Table 1. The lower heating value of pine sawdust ($\text{LHV}_{\text{biomass}}$) is approximately 19.80 MJ/kg.

2.2. Chemical reaction model

2.2.1. Two-step pyrolysis of biomass

The biomass pyrolysis in the two-step process can be described as following reactions (Li et al., 2019b):



The mass fraction of each product can be determined by the ultimate and proximate analyses of the pine sawdust in Table 1. According to the analyses results and literature (Li et al., 2019), the mass fractions are listed in Table 2.

2.2.2. Char gasification

Char gasification with CO_2 , namely the Boudouard reaction, take

Table 1
Ultimate and proximate analyses of pine sawdust (wt%) (Huang et al., 2013).

Ultimate analysis					Proximate analysis		
C _d	H _d	O _d	N _d	S _d	Volatiles	Fixed carbon	Ash
48.44	6.21	45.29	0.05	0.01	84.82	14.58	0.60

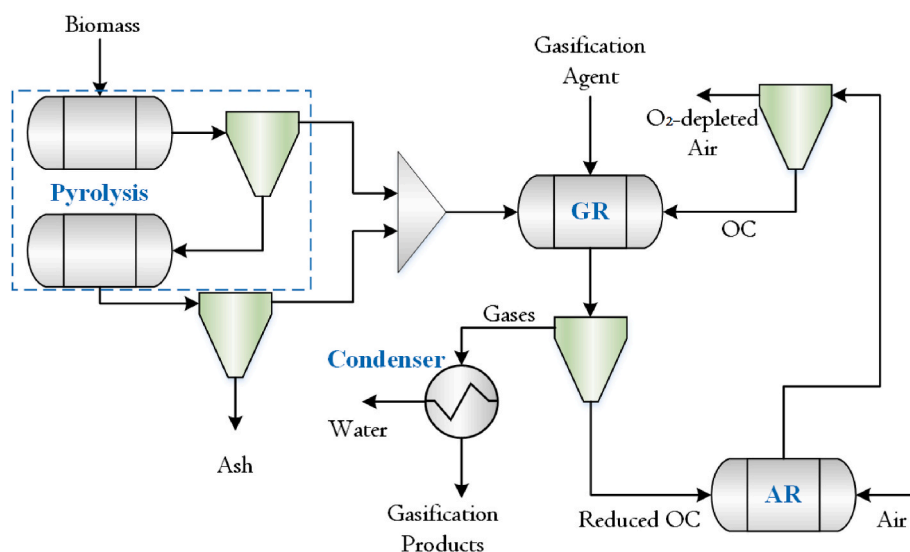


Fig. 1. Process model of CLG for biomass.

Table 2

Mass fraction of pyrolysis results in R1 and R2.

Reaction	Mass fraction								
	Char	CH ₄	C ₂ H ₄	CO	CO ₂	H ₂	H ₂ O	Tar	Tar _{inert} /ash
R1	0.147	0.078	0.037	0.456	0.183	0.016	0.010	0.073	–
R2	–	0.102	–	0.650	0.128	0.020	–	–	0.100

As the pyrolysis process is always fast at higher temperature, the reaction time and kinetics are not considered in this work.

place in gasifier, which is described as:



The reaction rate is related to the CO₂ and CO partial pressures, which is given as (Samprón et al., 2021):

$$r_{C,CO_2} = \frac{k_{CO_2} p_{CO_2}}{1 + K_{CO_2} p_{CO_2} + K_{CO} p_{CO}} (1 - X_C) \quad (1)$$

Here, X_C is the conversion of biomass char; p_{CO_2} and p_{CO} are partial pressures of CO₂ and CO respectively; The k_{CO_2} , K_{CO_2} and K_{CO} are kinetic constants which can be calculated using Arrhenius equation:

$$k_i = k_{0,i} e^{-\frac{E_{A,i}}{RT}} \quad (2)$$

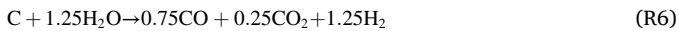
$$K_i = K_{0,i} e^{-\frac{\Delta H_i}{RT}} \quad (3)$$

where, k_0 and K_0 are pre-exponential factors; E_A and ΔH denote activation energies. Here, k_{0,CO_2} , K_{0,CO_2} and $K_{0,CO}$ are 1.3×10^3 / (bar · s), 3.9×10^{-5} / bar and 2.9×10^{-6} / bar, respectively. E_{A,CO_2} , ΔH_{CO_2} and ΔH_{CO} are 141.8, –112.7 and –154.7 kJ/mol, respectively (May et al., 2018).

The steam gasification and water-gas shift reaction also take place in gasification process:



They can be combined and reformed as following reaction (Ohle-müller et al., 2015):



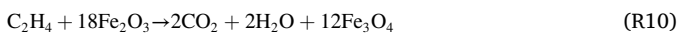
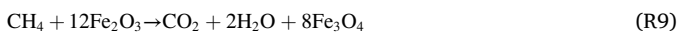
The reaction rate of R5 is calculated by

$$r_{C,H_2O} = \frac{k_{H_2O} p_{H_2O}}{1 + K_{H_2O} p_{H_2O} + K_{H_2} p_{H_2}} (1 - X_C) \quad (4)$$

where, p_{H_2O} and p_{H_2} are partial pressures of H₂O and H₂ respectively; The k_{H_2O} , K_{H_2O} and K_{H_2} are kinetic constants obtained using Equations (2) and (3). k_{0,H_2O} , K_{0,H_2O} and K_{0,H_2} are 1.1×10^3 / (bar · s), 4.1×10^{-4} / bar and 1.0×10^{-5} / bar, respectively. E_{A,CO_2} , ΔH_{CO_2} and ΔH_{CO} are 120.4, –88.3 and –151.9 kJ/mol, respectively (May et al., 2018).

2.2.3. Reduction of oxygen carrier

In GR, chemical looping gasification of biomass mainly is the reduction of Fe₂O₃. Related reactions are given as:



Fe₂O₃ can be reduced into Fe₃O₄, FeO and Fe. Usually, in CLG, it is always reduced to Fe₃O₄ and the FeO in following oxidation reaction could release large amount of heat, which may cause sintering of OC. Thereof, the reduced state of OC is considered as Fe₃O₄ and further reduction is not accounted into consideration in this work.

The reduction rates of reactions (R6) –(R9) are described by following equation (May et al., 2018):

$$r_{OC,i} = \frac{dX_{OC,i}}{dt} = \frac{3b_i k_i c_i^n}{\rho_m r_g} R_{OC} (1 - X_{OC,i})^{2/3} \quad (5)$$

Where, X_{OC} is the conversion of OC; R_{OC} is the practical oxygen transport capacity of OC, which is 3.33% of Fe₂O₃; ρ_m is molar density, 60,627 mol/m³; r_g is grain radius, 3.29×10^{-7} m; b_i denotes average stoichiometric coefficient of each reaction; c_i represents gas concentration and n is reaction order; k_i refers kinetic constant, which is calculated by Equation (2). Detailed values of these parameters are listed in Table 3.

3. Data processing

The conversion of the OC X_{OC} is defined as the molar ration of Fe in Fe₃O₄ to Fe in both Fe₂O₃ and Fe₃O₄, namely:

$$X_{OC} = \frac{3n_{Fe_3O_4}}{3n_{Fe_3O_4} + 2n_{Fe_2O_3}} \quad (6)$$

Here, $n_{Fe_3O_4}$ and $n_{Fe_2O_3}$ are molar of Fe₃O₄ and Fe₂O₃, respectively.

To evaluate the gas concentrations of main gasification products, the gas composition C_i is defined as:

$$C_i = \frac{n_i}{n_{H_2} + n_{CO} + n_{CO_2} + n_{CH_4} + n_{C_2H_4}} \quad (7)$$

where, n_i is the molar flow of each gas in the outlet of gasifier.

Total gas yield G_V is used to evaluate the volume flow of gas products, which is defined as:

$$G_V = \frac{22.4(n_{H_2} + n_{CO} + n_{CO_2} + n_{CH_4} + n_{C_2H_4})}{1000m_{biomass}} \quad (8)$$

in which, $m_{biomass}$ is the mass feeding rate of biomass.

Carbon conversion efficiency is used to evaluate the carbon fraction which has been converted from biomass to gaseous products, given as

$$\eta_C = \frac{12(n_{CO} + n_{CO_2} + n_{CH_4} + n_{C_2H_4})}{1000m_{biomass}f_C} \quad (9)$$

where, f_C is the mass fraction of carbon in biomass.

The LHV (MJ/Nm³) of produced gas can be calculated by following equation (Li et al., 2019):

$$LHV = 12.6C_{CO} + 10.8C_{H_2} + 35.9C_{CH_4} + 63.5C_{C_2H_4} \quad (10)$$

Gasification efficiency is defined as (Li et al., 2019):

Table 3

Values of rate parameters (May et al., 2018).

Parameter	CH ₄	H ₂	CO	Unit
b_i	5.78	1.45	1.45	–
n	1	1	0.8	–
$k_{0,i}$	9.8	0.062	0.1	mol ¹⁻ⁿ m ³ⁿ⁻² s ⁻¹
$E_{A,i}$	135.2	65	80.7	m

What should be noted that the kinetic parameters of (R9) are assumed to be same as those of (R8).

$$\eta = \frac{LHV \times G_V}{LHV_{biomass}} \quad (11)$$

4. Process simulation results and discussions

4.1. Process parameters and model validation

During the whole simulation process, the biomass, gasification agent and OC are continuously fed into the system. The yield reactor is adopted to simulate the two-step pyrolysis as it is a fast process as aforementioned. The GR is assumed as a plug flow reactor, whose diameter and length are 0.06 m and 0.70 m, which are same as the values in Ref (Huang et al., 2013). Under the fundamental condition, the operating parameters kept same as these in experiment of Ref (Huang et al., 2013). The argon gas molar flow is converted into molar flow, which is 0.061 mol/h. The volume flow of OC is convert into mass flow according to the density and Fe₂O₃ content in OC, which is 0.26 kg/h Fe₂O₃. The gasifier temperature is set as 840 °C. The biomass feeding rate is 0.12 kg/h in this case, the calculated and experimental results are listed in Table 4.

As illustrated in Table 4, the simulation results of gas compositions are of high agreement with those of experiment. It demonstrates that the established model can be used for the simulation of this CLG process. Thereof, this model is used for variable condition simulation in following parts. What should be noted is that the carbon conversion efficiency in simulation is less than that in experiment, but it is in the variation range of multi-cycle experimental results in Ref (Huang et al., 2013).

4.2. Effect of gasification temperature

The gasification temperature is a key factor in CLG. The referred experiment investigated the gasification performance at 840 °C. To evaluate its effects on CLG process, the gasification temperature is changed from 740 °C to 880 °C while other parameters are kept constant. The gas compositions under different gasification temperatures are shown in Fig. 2.

Results in Fig. 2 illustrate the molar flow of CO dramatically increases from 2.00 mol/h to 3.44 mol/h with the rising of gasification temperature from 740 °C to 880 °C. The H₂ molar flow also increases from 0.79 mol/h at 740 °C to 1.19 mol/h at 880 °C. Contrarily, the CO₂ molar flow shows decreasing trend, declining from 0.67 mol/h to 0.17 mol/h during this variation process. CH₄ and C₂H₄ decrease slightly with the reaction temperature. For gas compositions, they are similar with the variations of molar flow. The H₂ and CO compositions climb from 18.79% to 47.23%–21.49% and 62.18%, respectively. Meanwhile, CO₂ composition decreases from 15.95% to 3.00%. High temperature is beneficial to the endothermic Boudouard reaction expressed by (R3). On the contrary, it restrains the exothermic reaction of Fe₂O₃ reduction with CO. Thereof, the CO generation is intensified and conversion of CO to CO₂ is weakened simultaneously. As the steam gasification of char is also endothermic, higher temperature leads to the increase of H₂ composition in the gas phase. In addition, the molar ratio of H₂/CO shows decreasing trend when the temperature increases.

When the OC amount is kept constant, the increase of the temperature can enhance the conversion of OC. The mass and conversion of OC obtained from the stream of reduced OC are show in Fig. 3. As the temperature increases from 740 °C to 880 °C, the mass flow of Fe₂O₃ decreases from 0.038 to 0 kg/h while the mass of Fe₃O₄ rises from 0.215

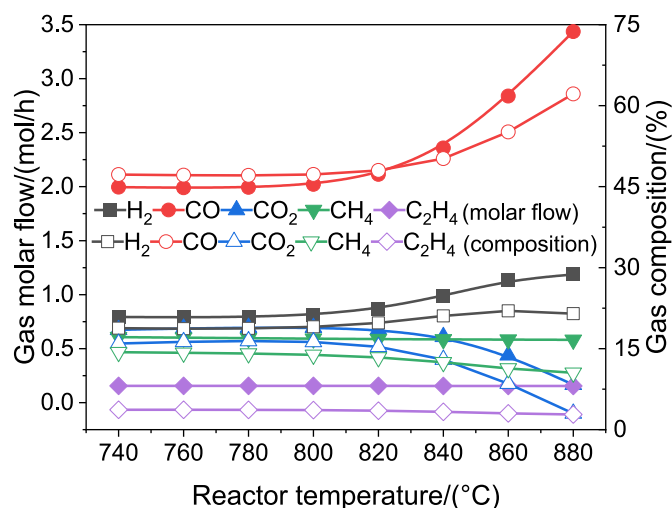


Fig. 2. Effect of gasification temperature on gas phase.

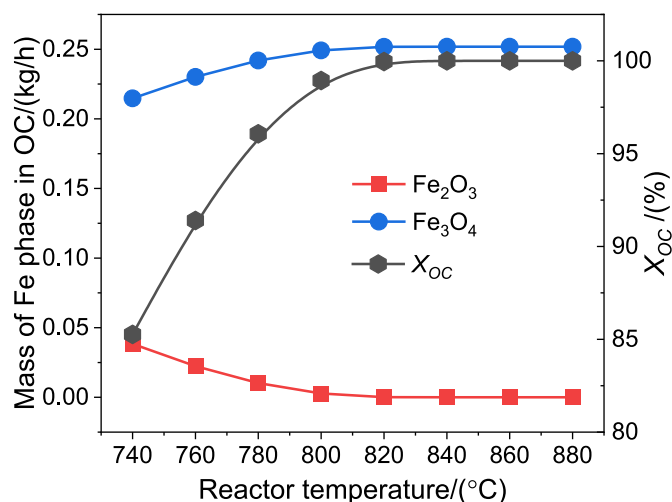


Fig. 3. Effect of gasification temperature on OC conversion.

to 0.252 kg/h. Meanwhile, the OC conversion X_{OC} climbs from 85.26% to 100%. From the curves, it can be found that the mass flow of Fe phases and OC conversion have reached stable values when the temperature is higher than 820 °C. The higher temperature can improve the biomass conversion to produce more CO while more oxygen should be provided by OC. Results also demonstrated that the OC conversion increases more sharply at lower temperature. However, it should be noted that in practical operation of a chemical looping unit, the OC conversion relates to many factors including operating parameters, reactor geometry, etc. It is one of the key factors which influence the OC lifetime. High OC conversion in single redox process is not beneficial to the OC lifetime.

The effects of gasification temperature on total gas yield, carbon conversion efficiency and gasification efficiency are given in Fig. 4.

Obviously, the total gas yield and efficiencies increase with the gasification temperature and the increment becomes larger at higher temperature. The total gas yield increases from 0.79 to 1.03 Nm³/kg when the temperature varies from 740 °C to 880 °C. More gas is produced in CLG process. The carbon conversion efficiency and gasification efficiency reach 92.76% and 81.87% from 74.05% to 61.62% respectively. The increasing carbon conversion is consistent with the climbing CO flow in Fig. 2. Results demonstrate that the endothermic biomass conversion are significantly enhanced at the escalating temperature. The higher CO and H₂ compositions at high temperature is beneficial to

Table 4

Comparison of calculated and experimental CLG results.

Item	C _{H2}	C _{CO}	C _{CO2}	C _{CH4}	C _{C2H4}
Simulation	21.06%	50.19%	12.98%	12.47%	3.30%
Experiment (Li et al., 2020)	21.97%	50.57%	11.58%	12.31%	3.57%

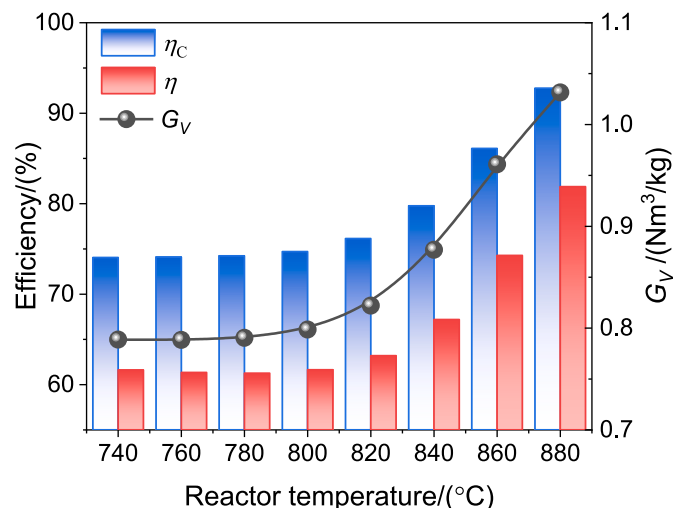


Fig. 4. Effect of gasification temperature on efficiencies and G_v .

improve the LHV of gasification products. Meanwhile, the total gas yield also increases against temperature, hence, the gasification efficiency decreases sharply at high temperature.

4.3. Effects of the mass flow of OC

During CLG process, the oxygen for gasification is provided by the lattice oxygen in OC. Definitely, the change of OC amount can influence the CLG performance of pine sawdust. To investigate its effects quantitatively, the OC amount is changed from 0 to 1.5 kg/h in established CLG process while other parameters are same with those under fundamental condition. In this case, the gasification products are shown in Fig. 5.

With the increase of OC mass flow in CLG, both of the molar flow and gas composition of combustible gases show decreasing trend while the molar flow and gas composition of CO₂ gradually increase to higher level. However, the decrease of C₂H₄ is very slight. The decreasing interval of combustible gases becomes smaller while the OC mass flow increases from 0 to 1.5 kg/h. The CO molar flow and composition decrease from 2.36 mol/h and 50.95% to 2.23 mol/h and 48.28%, respectively. Molar flow and composition of CH₄ fall from 0.63 mol/h and 13.62% to 0.52 mol/h and 11.20% correspondingly. Meanwhile, the molar flow and composition of CO₂ increase from 0.42 mol/h and 9.09% to 0.93 mol/h and 20.05%, respectively. The increment of CO₂ molar is larger than the total decrement of CO and CH₄, which demonstrates that

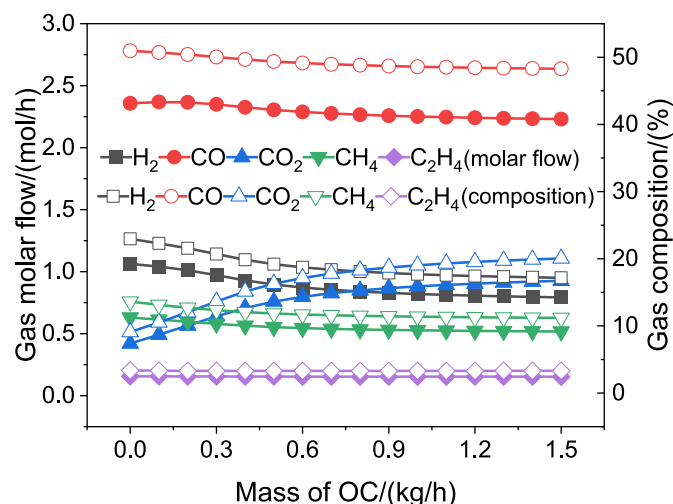


Fig. 5. Effect of OC mass flow on gas phase.

more carbon from biomass is converted.

The mass variations of Fe phases in OC and OC conversion are illustrated in Fig. 6.

As can be seen, both of the mass flowrates of Fe₂O₃ and Fe₃O₄ show ascending trend. Due to the continuous conversion of OC in CLG, the reduced OC Fe₃O₄ gradually increases from 0 to 0.643 kg/h while unconverted OC Fe₂O₃ rises from 0 to 0.838 kg/h. Definitely, the increased fresh OC into the system can not be totally converted. The consumed Fe₂O₃ takes a smaller proportion of the additive OC when the OC mass flow gets larger. Thereof, the curve of Fe₃O₄ tends to flat while that of Fe₂O₃ becomes more precipitous. Correspondingly, the OC conversion decreases against the mass flow of OC. While OC mass flow is no more than 0.3 kg/h, its conversion is 100%. When it further increases from 0.4 kg/h to 1.5 kg/h, the OC conversion decreases from 97.31% to 44.27%.

The total gas yield, carbon conversion efficiency and gasification efficiency are shown in Fig. 7 when the OC increases. As illustrated, the total gas yield increases at initial, then it decreases gradually. Interestingly, the maximum value of G_v occurs when the OC mass flow is 0.30 kg/h, which is also the critical value of $X_{OC} = 100\%$. The possible reason is that when the amount of OC further increases, more hydrogen or/and hydrocarbon is fully oxidized, and the product H₂O is condensed, causing the decrease of the gas yield. The carbon conversion efficiency and gasification efficiency have different variations when OC mass flow increases. The carbon conversion efficiency increases from 76.81% to 82.18% while the gasification efficiency decreases from 69.50% to 61.24%. The rise of OC can offer more lattice oxygen in CLG process, which improves the carbon conversion and enhances the combustion reactions (R6) to (R9). The increase rate of η_c becomes lower with the rise of OC amount. The lattice oxygen from OC continuously consumes the combustible gases, producing CO₂ and H₂O. That leads to the decrease of LHV of produced gas. As a comprehensive result of LHV and G_v , the gasification efficiency comes down gradually.

4.4. Effects of the molar flow of steam in gasification agent

Equation (4) demonstrates that the partial pressure of steam directly influences the gasification process of biomass char. To investigate its effect, the molar flow of steam is adjusted under the conditions of changed and unchanged total molar flow of gasification agent. When the total molar flow of gasification agent keeps unchanged as 0.061 mol/h, the molar flow of steam varies from 0.005 mol/h to 0.060 mol/h while other is argon. Further, the gasification agent is steam, varying from 0.060 mol/h to 0.760 mol/h with interval of 0.100 mol/h. The gas molar

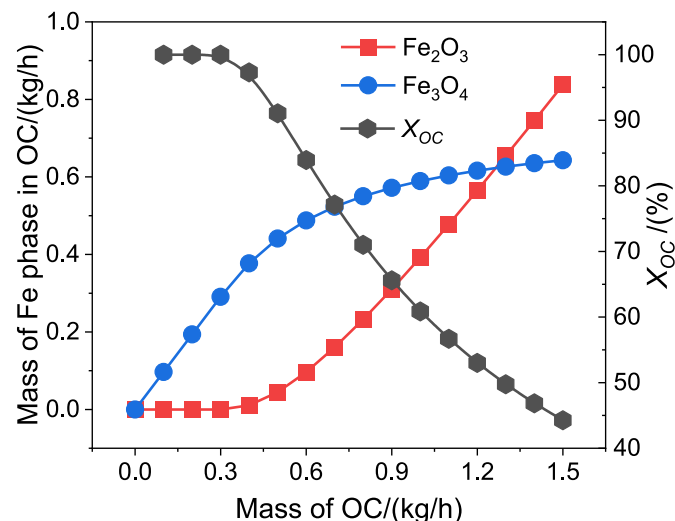


Fig. 6. Effect of OC mass flow on OC conversion.

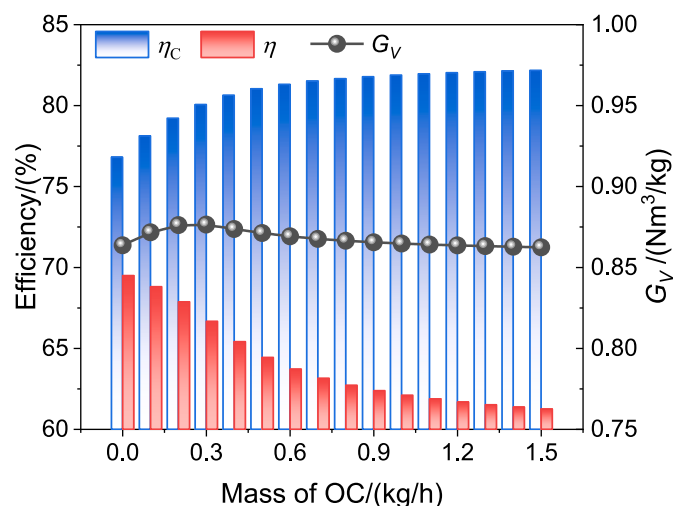


Fig. 7. Effect of OC mass flow on efficiencies and G_V .

flow and composition under these conditions are shown in Fig. 8.

When the molar flow of steam is no more than 0.060 mol/h, the variations of gas flow and compositions are quite slight. The gas flow and composition of H_2 slightly increases from 0.9919 mol/h and 21.09% to 1.0216 mol/h and 21.47%, respectively. The flow of CO increases from 2.3596 mol/h to 2.3789 mol/h while its composition declines from 50.17% to 50.00%. The increase of steam will rise the partial pressure of steam, which is beneficial to the steam gasification of char, enhancing the H_2 and CO production as illustrated in reaction (R5). Correspondingly, the consumption of H_2 and CO also accelerate expressed by reactions (R6) and (R7). The consumption rate is lower than the production, which leads to the increase of CO_2 molar flow while the CO_2 composition decreases. When the gasification agent is pure steam and increases with higher interval of 0.100 mol/h, the variation of gas is more obvious. The molar flow and gas composition of H_2 rise from 1.0712 mol/h and 22.11% to 1.3390 mol/h and 25.15% respectively when the steam molar flow increases from 0.160 mol/h to 0.760 mol/h. In this case, the CO molar flow increases from 2.4062 mol/h to 2.5534 mol/h while its compositions decrease from 49.65% to 47.95%. CH_4 molar flow shows a slightly increasing trend from 0.5865 to 0.5883 mol/h while its composition decreases from 12.10% to 11.05%.

Under these conditions, the oxygen carrier conversion reaches 100%, demonstrating a full reduction of Fe_2O_3 to Fe_3O_4 . The carbon conversion efficiency, gasification efficiency and gas yield are shown in Fig. 9.

As the steam gasification of biomass char is enhanced, the carbon conversion definitely increases while the steam molar flow rises. The carbon conversion efficiency is 79.81% when molar flow of steam is

0.005 mol/h; it reaches 80.32% and 85.48% while steam flow increases to 0.060 mol/h and 0.760 mol/h, respectively. It can be found that the total gas yield is linearly related to the molar flow of steam approximately. The total gas yield increases from 0.8778 mol/h to 0.9940 mol/h when the steam molar flow goes up from 0.005 mol/h to 0.760 mol/h. The gasification efficiency is 67.24% when the steam flow is 0.005 mol/h. It further increases to 67.78% and 73.15% when steam flow rises to 0.060 mol/h and 0.760 mol/h, respectively.

4.5. Coupled effects of the amounts of OC and steam

In a practical CLG system, the variation of operating condition may be complex due to the simultaneous change of multiple parameters. The amounts of OC and steam in CLG process are changed simultaneously to investigate their coupled effects on the gasification performance. The gasification agent is set as pure steam without dilution by argon. The gas compositions in this case are shown in Fig. 10.

Under the variable conditions shown in the figure, the H_2 composition and CO_2 composition have the largest variation ranges. As can be seen, increasing the steam flow and decreasing the OC mass are beneficial to the H_2 production. The maximum and minimum H_2 compositions are 28.22% and 17.69% when the steam and OC flow are (1.0 mol/h, 0 kg/h) and (0 mol/h, 1.0 kg/h), respectively. When the mass flow of OC is higher than 0.27 kg/h, the effect of steam molar flow (from zero to 0.59 mol/h) is dominant; when the molar flow of steam is more than 0.32 mol/h, the effect of OC mass flow (from zero to 0.38 kg/h) is dominant. With the increase of steam molar flow, the CO composition in produced gas decreases gradually. Similarly, the increase of OC mass flow also makes the CO composition decline. That is because the OC can react with CO and H_2 , lead to high consumption. Therefore, the CO_2 composition certainly gets higher when OC amount increases, which is consistent with the result in Fig. 10(c). The CO_2 flowrate affected by the increase of steam flowrate is very obvious when the OC mass flow is near 1.0 kg/h. But the effect of steam on that is quite weak when OC mass flow is in the range from 0.2 to 0.4 kg/h. As steam gasification of char can notably enhance the H_2 production, the gas composition of CO_2 decreases against the steam flow. However, the steam molar flow has different effects on CO_2 composition when the OC amount are different. While OC amount is lower than 0.25 kg/h, the increase of steam molar flow can rise the CO_2 composition; while OC amount is higher, the steam flow has negative effect on the CO_2 composition. The OC mass flow and steam molar flow have similar effects on the CH_4 composition, that is, the increase of OC or steam can reduce the CH_4 composition. The variation of C_2H_4 should be caused by divergent gas yields under different conditions.

When the amounts of OC and steam are changed simultaneously, the X_{OC} result is shown in Fig. 11. The OC conversion decreases against its mass flow. Under a specific mass flow of biomass, the biomass char is

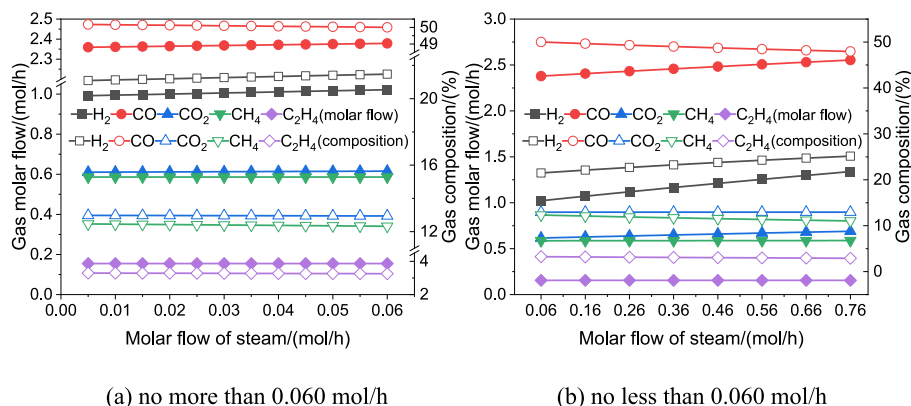


Fig. 8. Effect of steam molar flow in gasification agent on the gas phase.

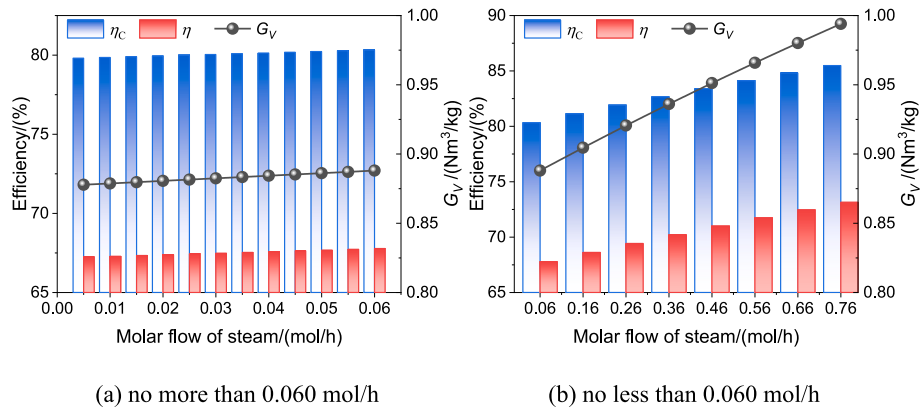


Fig. 9. Effect of steam molar flow in gasification agent on efficiencies and G_v .

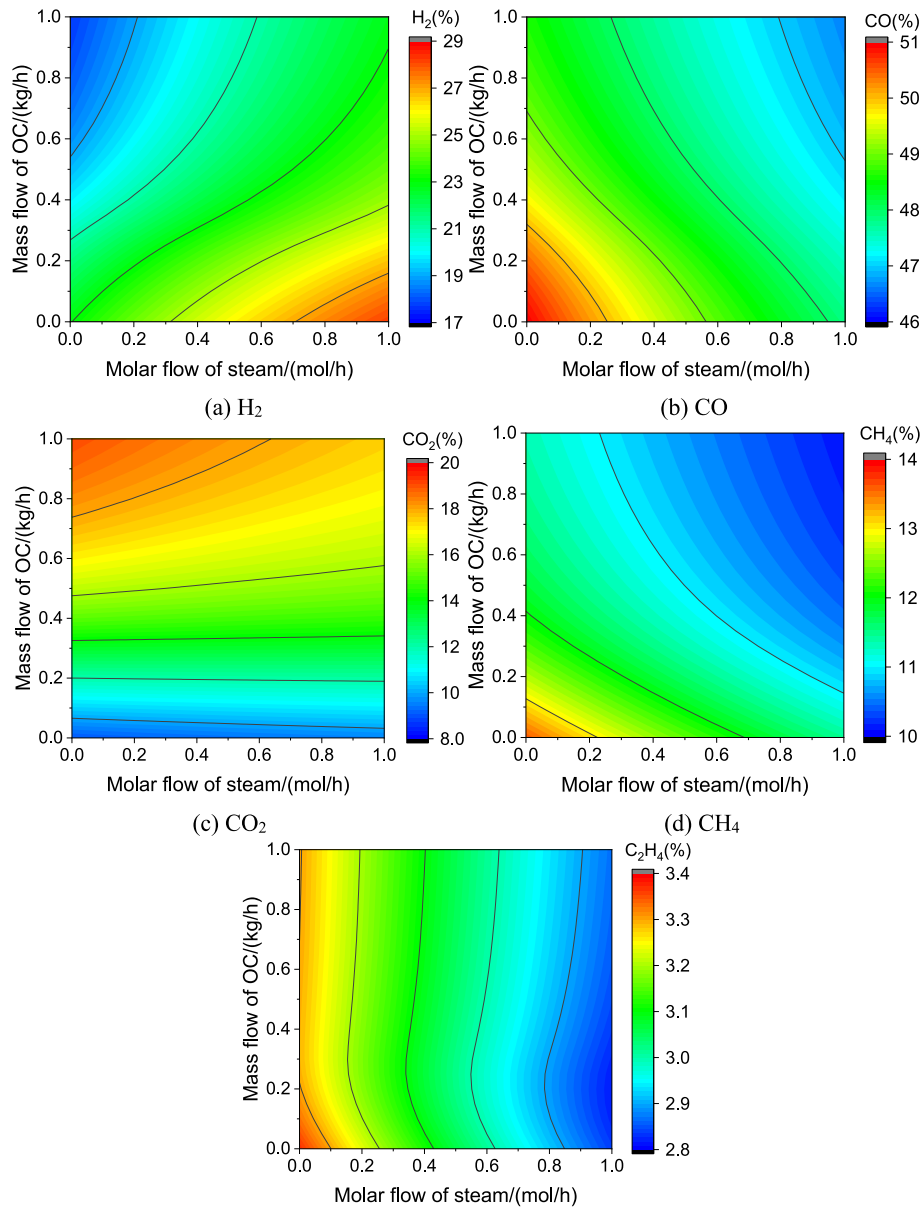


Fig. 10. Coupled effect of the amounts of OC and steam on gas compositions.

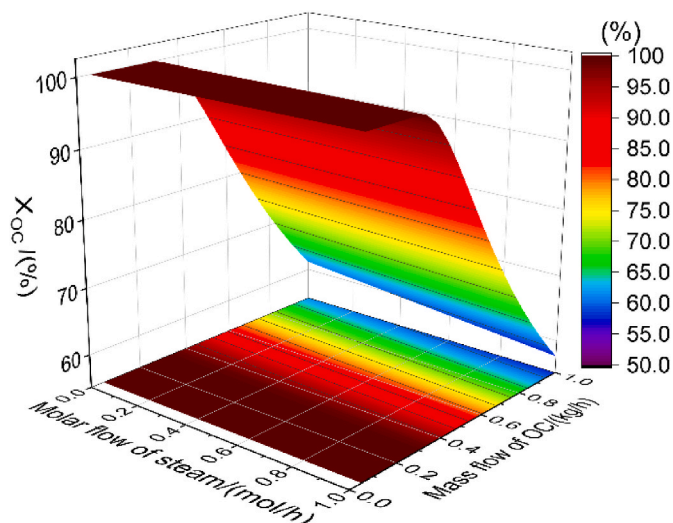


Fig. 11. Coupled effect of the amounts of OC and steam on OC conversion.

determined. Increasing the OC can consume more Fe_2O_3 in the OC, converting it to Fe_3O_4 . However, as the converted Fe_3O_4 is less than the increase rate of OC, the OC conversion X_{OC} shows a declining trend. When the mass flow of OC is less than 0.3 kg/h, the X_{OC} is almost 100% while the steam flow varies. When the OC mass flow is specific, increasing the molar flow of steam can result in the decrease of OC conversion. When the OC and steam flows are 1 kg/h and 1 mol/h, the X_{OC} is the lowest, which is 57.59%.

The coupled effect of OC and steam on the carbon conversion efficiency is shown in Fig. 12. With the increase of steam and OC amount, the carbon conversion is enhanced definitely. When there is no OC, the carbon conversion efficiency increases from 76.84% to 84.68% while the molar flow of steam rises from 0 to 1.0 mol/h; When these is no steam introduced into the CLG system, the carbon conversion efficiency rises from 76.84% to 82.00% as the mass of OC climbs from 0 to 1.0 kg/h. The figure also illustrates that the effect of the steam increment of 0.1 mol/h on carbon conversion is much more significant than that of the OC increment of 0.1 kg/h. When both of them increases from 0 to 1.0 kg/h or 1.0 mol/h, the carbon conversion efficiency reaches the maximum value of 88.57%. The reason for this phenomenon is that the steam gasification process can be intensified while more steam is

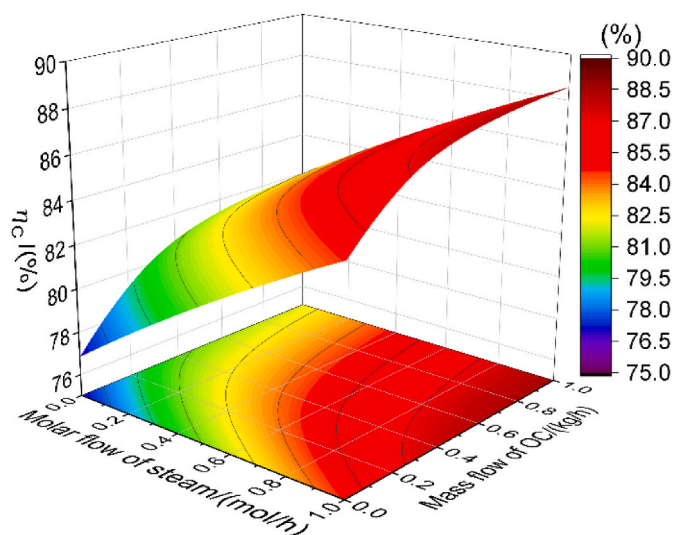


Fig. 12. Coupled effect of the amounts of OC and steam on carbon conversion efficiency.

introduced the system while OC can enhance the conversion of combustible gas resulting higher rates expressed by Equations (1) and (4).

The gasification efficiency against the OC and steam amount is shown in Fig. 13. The variations of steam and OC have opposite influence on the gasification efficiency. In detail, the increase of steam molar flow is positively related to the gasification efficiency while it is contrary of the effect of OC mass flow. Thereof, the minimum and maximum values of gasification efficiencies are 62.13% and 77.73% when the amounts of steam and OC are (0 mol/h, 1.0 kg/h) and (1.0 mol/h, 0 kg/h), respectively. The increase of steam in CLG is beneficial to produce more combustible gas H_2 . However, the increase of OC mass can consume more combustible gases, producing CO_2 or H_2O . This reduces the LHV of gasification product, resulting in the decrease of gasification efficiency.

4.6. Coupled effects of the gasification temperature and amount of OC

As demonstrated in previous section, the effect of a specific operating parameter also depends on the range of other parameters. In this section, the coupled effects of gasification temperature and mass flow of OC are investigated. When they are simultaneously changed, the OC conversion, carbon conversion efficiency and gasification efficiency are shown as Fig. 14, 15 and 16.

In the operating parameter setting, there is no steam in the reactor under these conditions while argon is used as carrying gas. When the amount of OC is low, it is seen that OC is totally converted to offer lattice oxygen for CLG. With the increase of OC amount, the OC conversion shows decreasing trend. When the mass flow of OC increases from 0.1 kg/h to 1.0 kg/h, the decline range of OC conversion is different while temperature changes. That demonstrates the coupled effects of these operating parameters. When the temperature is 750 °C, the OC conversion decreases from 100% to 34.04% while mass flow of OC increases from 0.1 kg/h to 1.0 kg/h. The OC conversion decreases from 100% to 64.92% at 850 °C. Increasing OC mass flow at any temperature can enhance the conversion of combustible gases, which leads to the increasing of CO_2 composition and decreasing of CO , H_2 , CH_4 and C_2H_4 . It can be demonstrated by the gas composition results Fig. S1 in Supplementary Material. At low temperature, the conversion of biomass is restricted, thereof, less oxygen is needed which leads to a low OC conversion. When the temperature climbs, char gasification process is intensified. Meanwhile, the conversion of combustible gases in gasification products is also enhanced. The oxygen in these processes is from

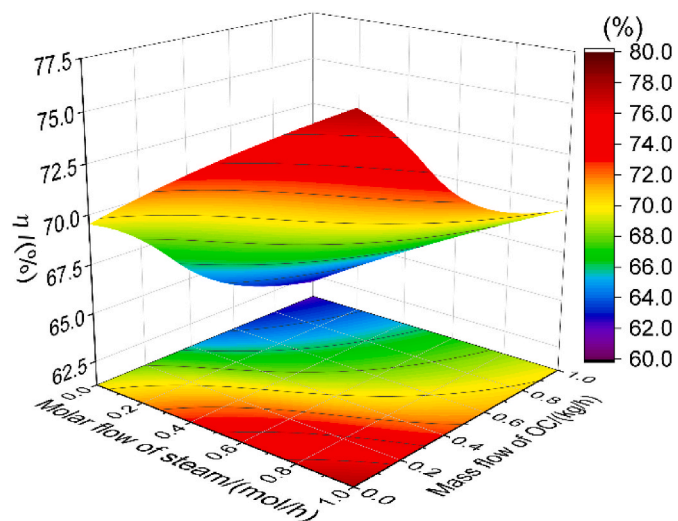


Fig. 13. Coupled effect of the amounts of OC and steam on gasification efficiency.

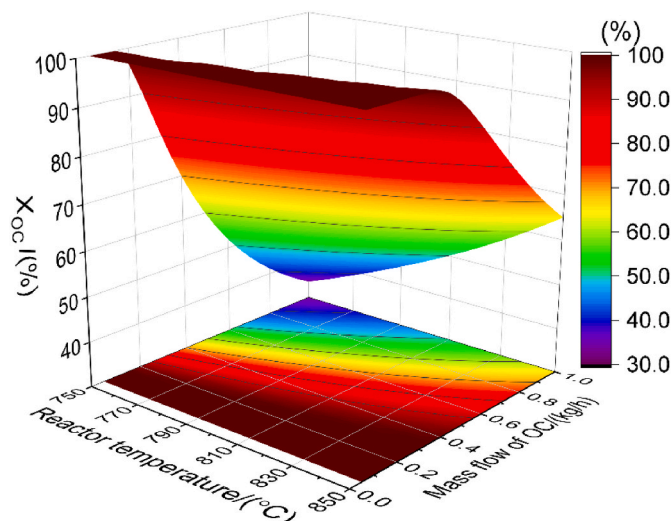


Fig. 14. Coupled effect of the temperature and amount of OC on OC conversion.

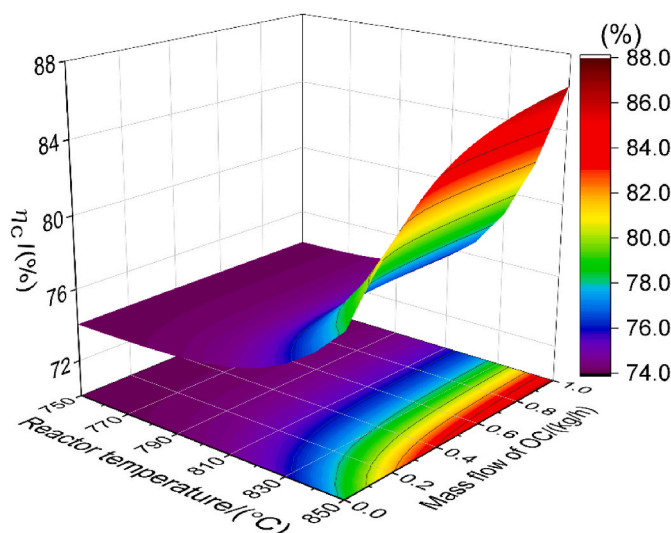


Fig. 15. Coupled effect of the temperature and amount of OC on carbon conversion efficiency.

OC. Thereof, the OC conversion increases against reactor temperature. This is also the reason why OC conversion of 100% takes a higher proportion at 850 °C when OC mass flow changes.

The carbon conversion efficiency definitely increases with the climbing of temperature and OC mass flow. However, when the temperature is lower than 810 °C, the enhancement effect of temperature and OC mass flow is quite slight. When it is higher than 810 °C, the carbon conversion efficiency dramatically increases against the reaction temperature, especially when the mass flow of OC is at a high level. When mass flow of OC is zero, the carbon conversion efficiencies are 74.05% at 750 °C and 78.31% at 850 °C; and they are 74.07% and 86.32% respectively, when OC mass flow is 1.0 kg/h. To explain the result, the carbon conversion is mainly related to the gasification reactions between carbon and CO₂ or steam. Meanwhile, the concentrations of CO₂ and steam are determined by gasification reactions and conversion of combustible gases. Increasing temperature is beneficial to the gasification process and conversion of combustible gases while more oxygen for gasification can be offered with a higher mass flow of OC.

Different from carbon conversion efficiency, the gasification efficiency shows decreasing trend against the mass flow of OC. As the

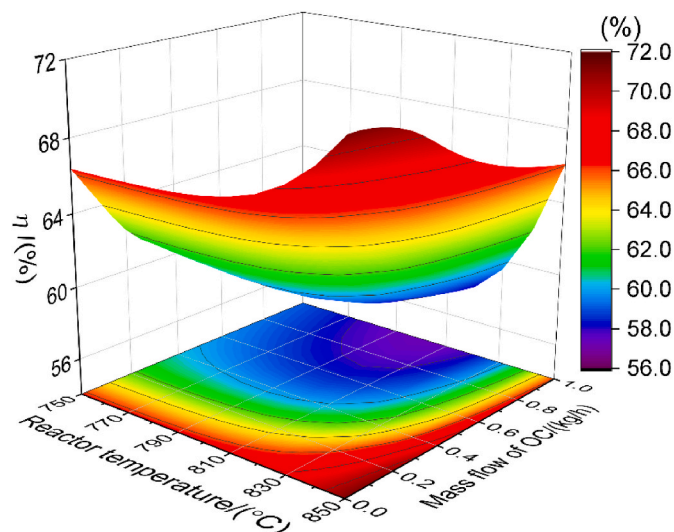


Fig. 16. Coupled effect of the temperature and amount of OC on gasification efficiency.

gasification efficiency is a comprehensive result of gas yield and lower heating value, when OC mass flow increases, more oxygen is offered for gasification, leading to the gas yield in some extent. However, it enhances the conversion of combustible gases, which leads to the increase of CO₂ in products and decrease of other gases. In this sense, the lower heating value of the gasification products decreases against the OC mass flow. As its effect on heating value reduction overtakes that on gas yield, the gasification efficiency decreases with the increase of OC mass flow. When the reactor is operated at 750 °C and 850 °C, the gasification efficiency decreases from 66.39% to 71.21%–59.10% and 66.11% respectively. Though increasing temperature is beneficial to the gasification process, it can also enhance the conversion of combustible gases. Additionally, the temperature can affect the reverse reaction of water-gas shift reaction. When the OC mass flow is not sufficient, increasing temperature can promote the gasification efficiency. When OC mass flow further increases, the OC can convert the CO, H₂ to CO₂ and H₂O. In this case, the gas composition of CO₂ increases against temperature, which is exhibited as Fig. S1 in Supplementary Material. As steam is condensed, aforementioned result leads to the decline of gas yield and lower heating value simultaneously. The minimum value of gas yield occurs approximately 800 °C. When the temperature further increases, the compositions of H₂ and CO become larger and that of CO₂ decreases, which can enhance the gasification efficiency.

4.7. Coupled effects of the gasification temperature and steam

When the OC mass flow is fixed as the value in fundamental condition, the reactor temperature and molar flow of steam are changed simultaneously to investigate their effects on the CLG performances. The results of related indexes are shown in Fig. 17, 18 and 19.

In this case, the OC amount is constant while steam flow varies from 0 to 1.0 mol/h while the temperature increases, the conversion of combustible gases definitely improve the OC conversion. When the molar flow of steam keeps constant, increasing temperature can enhance the gasification process and conversion of combustible gases, which is shown as Fig. S2 in Supplementary Material. Additionally, the CO₂ first increases and then decreases against the temperature. This is the comprehensive result of aforementioned processes. Both of them can enhance the conversion of OC. When it is 750 °C, the OC conversion is 88.48% under the condition of steam-free CLG. The conversion reaches 100% when the temperature rises to 850 °C. As has been mentioned in previous part, the oxygen in CLG is offered by OC and steam. When the steam molar flow increases, the OC conversion shows decreasing trend,

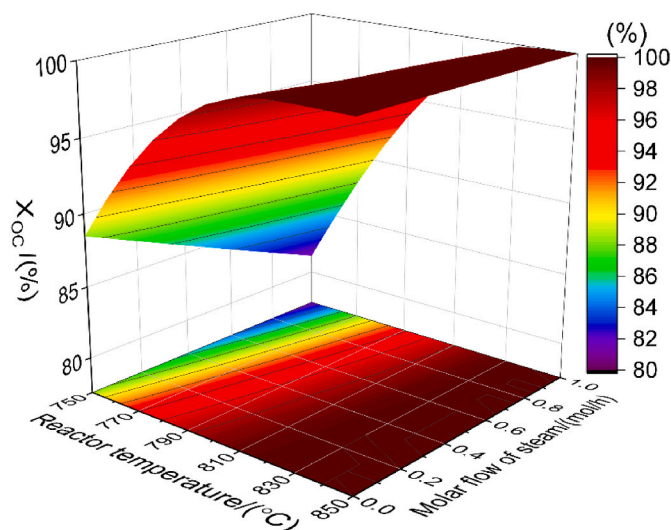


Fig. 17. Coupled effect of the temperature and steam on OC conversion.

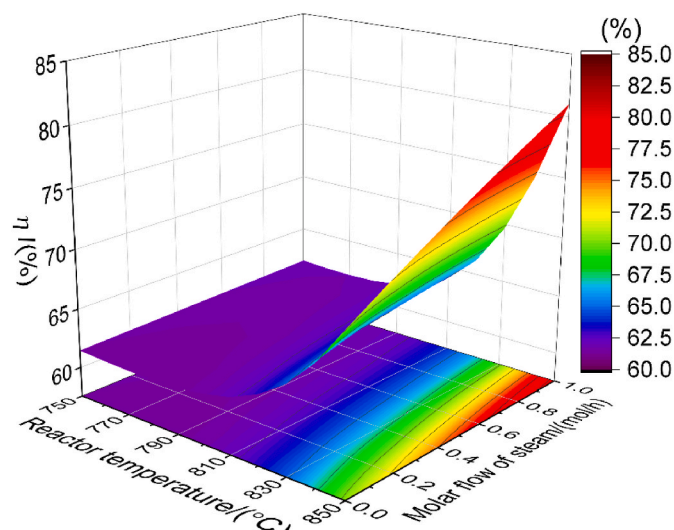


Fig. 19. Coupled effect of the temperature and steam on gasification efficiency.

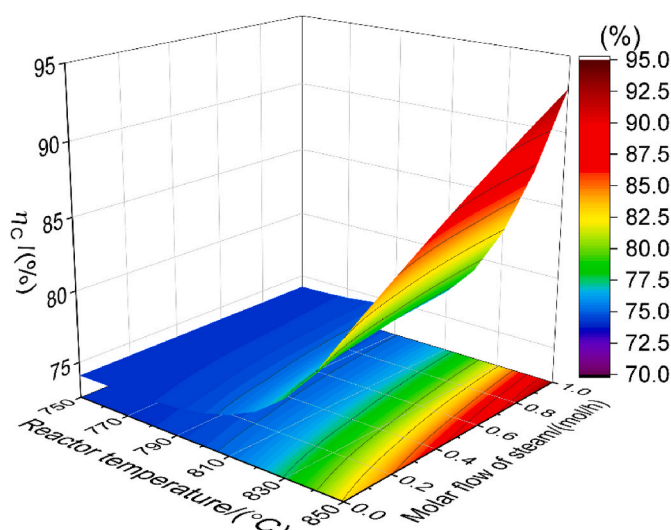


Fig. 18. Coupled effect of the temperature and steam on carbon conversion efficiency.

especially at lower temperature. When the temperature is 750 °C, the OC conversion decreases from 88.48% to 81.32% while steam flow varies from 0 to 1.0 mol/h. The OC conversion of 81.32% is also the minimum value in this case. At a higher temperature, the gasification products can be easily converted into CO₂ and H₂O by OC. Thereof, the OC conversion is in a quite high level at high temperature range.

Carbon conversion is mainly reflected by the char gasification. It is seen that the carbon conversion efficiency increases slightly against temperature when the temperature is lower than 810 °C. In that range, though increasing steam flow can enhance the carbon conversion, its effect is also quite slight. That means the gasification rate in that range is low though the temperature and steam concentration can enhance it. When the temperature is higher than 810 °C, effect of increasing temperature on carbon conversion efficiency becomes conspicuous. The increasing of steam molar flow can improve the char gasification process. It increases the partial pressure of gasification agent in the reactor, leading to the rise of reaction rate. At lower temperature, increasing the steam flow also has slight effect on carbon conversion efficiency. In that range, the temperature takes dominant role in the determination of carbon conversion.

As the changes of temperature and steam flow has slight effect on the carbon conversion in the low-temperature range, its effect on gasification efficiency is also not significant in the same case. Increasing steam molar flow can enhance the gasification process. As its oxidation ability is weaker than OC, it has no effect on the conversion of combustible gases. That is different from OC. Therefore, its increase can promote the gasification efficiency. At 750 °C, increasing steam molar flow from 0 to 1.0 mol/h can improve the gasification efficiency from 61.46% to 61.91% while gasification efficiency increases from 70.42% to 81.03% at 850 °C. When the steam flow is low, increasing temperature has less effect on gasification efficiency than that in high-steam flow range.

5. Conclusions

Chemical looping gasification can produce high-purity syngas without the necessity of extra purification process, which offers a more sustainable and cleaner disposal way for biomass comparing with traditional gasification. The simulation model of a laboratory-scale CLG setup is constructed and validated. According to the experimental conditions, this model is developed as a continuous biomass feeding CLG process model. Different operating parameters are changed to investigate their effects on gasification performances. From the results, following conclusions can be drawn:

- (1) Gasification temperature can greatly enhance the carbon conversion and gasification efficiencies upon 780 °C. When it is 880 °C, carbon conversion efficiency and gasification efficiency reach 92.76% and 81.87%. The OC conversion reach 100% when the temperature is higher than 820 °C.
- (2) Increasing OC mass flow from 0 to 1.5 kg/h causes the decrease of H₂, CO and CH₄ compositions, leading to the declination of gasification efficiency from 69.50% to 61.24%; however, the carbon conversion efficiency rises from 76.81% to 82.18%.
- (3) The steam gasification of biomass char is enhanced when steam flow rises. Correspondingly, the carbon conversion efficiency, gasification efficiency and total gas yield come up against the amount of steam.
- (4) The simultaneous variation of the amounts of OC and steam has coupled effects on the CLG performances. The minimum and maximum values of gasification efficiencies are 62.13% and 77.73% when the amounts of steam and OC are (0 mol/h, 1.0 kg/h) and (1.0 mol/h, 0 kg/h), respectively. When both of them

increases to 1.0 kg/h or 1.0 mol/h, the carbon conversion efficiency reaches the maximum value of 88.57%.

- (5) The coupled effects of temperature and OC or steam amount demonstrate that the carbon conversion efficiency is mainly determined by temperature at lower-temperature range. When temperature is higher than 810 °C, the effect of each parameter is conspicuous. Though both of OC and steam can offer oxygen in CLG, due to the different oxidation ability, their effects on gasification efficiency are opposite.

Investigating coupled effects in CLG technology is beneficial to develop this cleaning technology with high efficiency. Results can be further used to optimize the operating parameters of CLG system to realize an optimal performance or desirable gas compositions for downstream industry. Additionally, improvement of system design can be conducted based on the CLG model in this work, which will be investigated in future work.

CRedit authorship contribution statement

Shuaijie Xue: Methodology, Formal analysis, Writing – original draft. **Xudong Wang:** Conceptualization, Methodology, Formal analysis, Writing – original draft, Writing-Reviewing, Supervision.

Declaration of competing interest

The authors declare that they have no known competing financial interests or personal relationships that could have appeared to influence the work reported in this paper.

Acknowledgement

This work has been financially supported by China Postdoctoral Science Foundation (No. 2020M681455), Jiangsu Planned Projects for Postdoctoral Research Funds and the Fundamental Research Funds for the Central Universities.

Appendix A. Supplementary data

Supplementary data to this article can be found online at <https://doi.org/10.1016/j.jclepro.2022.131839>.

References

- Adán, J., Abad, A., Mendiara, T., Gayán, P., de Diego, L.F., García-Labiano, F., 2018. Chemical looping combustion of solid fuels. *PROG ENERG COMBUST* 65, 6–66.
- Cao, Y., He, B., Yan, L., 2019. Process simulation of a dual fluidized bed chemical looping air separation with Mn-based oxygen carrier. *ENERG CONVERS MANAGE* 196, 286–295.
- Condori, O., García-Labiano, F., de Diego, L.F., Izquierdo, M.T., Abad, A., Adán, J., 2021. Biomass chemical looping gasification for syngas production using ilmenite as oxygen carrier in a 1.5 kWth unit. *Chem. Eng. J.* 405, 126679.
- Darmawan, A., Ajiwibowo, M.W., Yoshikawa, K., Aziz, M., Tokimatsu, K., 2018. Energy-efficient recovery of black liquor through gasification and syngas chemical looping. *APPL ENERG* 219, 290–298.
- Deng, Z., Jin, B., Zhao, Y., Gao, H., Huang, Y., Luo, X., Liang, Z., 2018. Process simulation and thermodynamic evaluation for chemical looping air separation using fluidized bed reactors. *ENERG CONVERS MANAGE* 160, 289–301.
- Detchusanand, T., Im-orb, K., Maréchal, F., Arpornwathan, A., 2020. Analysis of the sorption-enhanced chemical looping biomass gasification process: performance assessment and optimization through design of experiment approach. *Energy* 207, 118190.
- Ge, H., Guo, W., Shen, L., Song, T., Xiao, J., 2016. Biomass gasification using chemical looping in a 25 kWth reactor with natural hematite as oxygen carrier. *Chem. Eng. J.* 286, 174–183.
- Gopaul, S.G., Dutta, A., Clemmer, R., 2014. Chemical looping gasification for hydrogen production: a comparison of two unique processes simulated using ASPEN Plus. *INT J HYDROGEN ENERG* 39, 5804–5817.
- He, F., Galinsky, N., Li, F., 2013. Chemical looping gasification of solid fuels using bimetallic oxygen carrier particles – feasibility assessment and process simulations. *INT J HYDROGEN ENERG* 38, 7839–7854.
- He, F., Huang, Z., Wei, G., Zhao, K., Wang, G., Kong, X., Feng, Y., Tan, H., Hou, S., Lv, Y., Jiang, G., Guo, Y., 2019. Biomass chemical-looping gasification coupled with water/CO₂-splitting using NiFe₂O₄ as an oxygen carrier. *ENERG CONVERS MANAGE* 201, 112157.
- Hu, J., Li, C., Guo, Q., Dang, J., Zhang, Q., Lee, D., Yang, Y., 2018. Syngas production by chemical-looping gasification of wheat straw with Fe-based oxygen carrier. *BIORESOUR TECHNOL* 263, 273–279.
- Hu, J., Li, C., Lee, D., Guo, Q., Zhao, S., Zhang, Q., Li, D., 2019. Syngas production from biomass using Fe-based oxygen carrier: Optimization. *BIORESOUR TECHNOL* 280, 183–187.
- Hu, Q., Shen, Y., Chew, J.W., Ge, T., Wang, C., 2020. Chemical looping gasification of biomass with Fe₂O₃/CaO as the oxygen carrier for hydrogen-enriched syngas production. *Chem. Eng. J.* 379, 122346.
- Huang, Z., Deng, Z., Chen, D., He, F., Liu, S., Zhao, K., Wei, G., Zheng, A., Zhao, Z., Li, H., 2017. Thermodynamic analysis and kinetic investigations on biomass char chemical looping gasification using Fe-Ni bimetallic oxygen carrier. *Energy* 141, 1836–1844.
- Huang, Z., He, F., Feng, Y., Zhao, K., Zheng, A., Chang, S., Li, H., 2013. Synthesis gas production through biomass direct chemical looping conversion with natural hematite as an oxygen carrier. *BIORESOUR TECHNOL* 140, 138–145.
- Huang, Z., Jiang, H., He, F., Chen, D., Wei, G., Zhao, K., Zheng, A., Feng, Y., Zhao, Z., Li, H., 2016a. Evaluation of multi-cycle performance of chemical looping dry reforming using CO₂ as an oxidant with Fe-Ni bimetallic oxides. *J. Energy Chem.* 25, 62–70.
- Huang, Z., Zhang, Y., Fu, J., Yu, L., Chen, M., Liu, S., He, F., Chen, D., Wei, G., Zhao, K., Zheng, A., Zhao, Z., Li, H., 2016b. Chemical looping gasification of biomass char using iron ore as an oxygen carrier. *INT J HYDROGEN ENERG* 41, 17871–17883.
- Li, G., Chang, Y., Chen, L., Liu, F., Ma, S., Wang, F., Zhang, Y., 2020. Process design and economic assessment of butanol production from lignocellulosic biomass via chemical looping gasification. *BIORESOUR TECHNOL* 316, 123906.
- Li, Z., Xu, H., Yang, W., Xu, M., Zhao, F., 2019a. Numerical investigation and thermodynamic analysis of syngas production through chemical looping gasification using biomass as fuel. *Fuel* 246, 466–475.
- Li, Z., Xu, H., Yang, W., Zhou, A., Xu, M., 2019b. CFD simulation of a fluidized bed reactor for biomass chemical looping gasification with continuous feedstock. *ENERG CONVERS MANAGE* 201, 112143.
- Lin, Y., Wang, H., Wang, Y., Huo, R., Huang, Z., Liu, M., Wei, G., Zhao, Z., Li, H., Fang, Y., 2020a. Review of biomass chemical looping gasification in China. *ENERG FUEL* 34, 7847–7862.
- Lin, Y., Wang, H., Huang, Z., Liu, M., Wei, G., Zhao, Z., Li, H., Fang, Y., 2020b. Chemical looping gasification coupled with steam reforming of biomass using NiFe₂O₄: kinetic analysis of DAEM-TI, thermodynamic simulation of OC redox, and a loop test. *Chem. Eng. J.* 395, 125046.
- Man, Y., Hu, S., Gao, J., Li, J., Hong, M., 2020. Integrated chemical looping combustion in pulp mill for high energy efficiency and low carbon emission. *J. Clean. Prod.* 275, 122979.
- May, J., Alobaid, F., Ohlemüller, P., Strohm, A., Ströhle, J., Eppe, B., 2018. Reactive two-fluid model for chemical-looping combustion -Simulation of fuel and air reactors. *INT J GREENH GAS CON* 76, 175–192.
- Mohamed, U., Zhao, Y., Huang, Y., Cui, Y., Shi, L., Li, C., Pourkashanian, M., Wei, G., Yi, Q., Nimmo, W., 2020. Sustainability evaluation of biomass direct gasification using chemical looping technology for power generation with and w/o CO₂ capture. *Energy* 205, 117904.
- Nurdiawati, A., Zaini, I.N., Irahmana, A.R., Sasongko, D., Aziz, M., 2019. Novel configuration of supercritical water gasification and chemical looping for highly-efficient hydrogen production from microalgae. *Renew. Sustain. Energy Rev.* 112, 369–381.
- Ohlemüller, P., Alobaid, F., Gunnarsson, A., Ströhle, J., Eppe, B., 2015. Development of a process model for coal chemical looping combustion and validation against 100 kWth tests. *APPL ENERG* 157, 433–448.
- Samprón, I., de Diego, L.F., García-Labiano, F., Izquierdo, M.T., 2021. Optimization of synthesis gas production in the biomass chemical looping gasification process operating under auto-thermal conditions. *Energy* 226, 120317.
- Samprón, I., de Diego, L.F., García-Labiano, F., Izquierdo, M.T., Abad, A., Adán, J., 2020. Biomass Chemical Looping Gasification of pine wood using a synthetic Fe₂O₃/Al₂O₃ oxygen carrier in a continuous unit. *BIORESOUR TECHNOL* 316, 123908.
- Sarafraz, M.M., Christo, F.C., 2020. Thermodynamic assessment and techno-economic analysis of a liquid indium-based chemical looping system for biomass gasification. *ENERG CONVERS MANAGE* 225, 113428.
- Sarafraz, M.M., Christo, F.C., 2021. Sustainable three-stage chemical looping ammonia production (3CLAP) process. *ENERG CONVERS MANAGE* 229, 113735.
- Stenberg, V., Rydén, M., Mattisson, T., Lyngfelt, A., 2018. Exploring novel hydrogen production processes by integration of steam methane reforming with chemical-looping combustion (CLC-SMR) and oxygen carrier aided combustion (OCAC-SMR). *INT J GREENH GAS CON* 74, 28–39.
- Sun, Z., Aziz, M., 2021. Comparative thermodynamic and techno-economic assessment of green methanol production from biomass through direct chemical looping processes. *J. Clean. Prod.* 321, 129023.
- Udomsirikakorn, J., Salam, P.A., 2014. Review of hydrogen-enriched gas production from steam gasification of biomass: the prospect of CaO-based chemical looping gasification. *Renew. Sustain. Energy Rev.* 30, 565–579.
- Wang, H., Liu, G., Veksha, A., Dou, X., Giannis, A., Lim, T.T., Lisak, G., 2021. Iron ore modified with alkaline earth metals for the chemical looping combustion of municipal solid waste derived syngas. *J. Clean. Prod.* 282, 124467.
- Wang, X., Wang, X., Zhang, S., Kong, Z., Jin, Z., Shao, Y., Jin, B., 2018a. Test operation of a separated-gasification chemical looping combustion system for coal. *ENERG FUEL* 32, 11411–11420.

- Wang, X., Wang, X., Shao, Y., Jin, Z., Jin, B., 2018b. Reactivity of a Chinese lean iron ore as oxygen carrier: kinetics and characterization. *Thermochim. Acta* 670, 114–122.
- Wang, X., Wang, X., Kong, Z., Shao, Y., Jin, B., 2020a. Auto-thermal operation and optimization of coal-fueled separated gasification chemical looping combustion in a pilot-scale unit. *Chem. Eng. J.* 383, 123159.
- Wang, X., Wang, X., Shao, Y., Jin, B., 2020b. Coal-fueled separated gasification chemical looping combustion under auto-thermal condition in a two-stage reactor system. *Chem. Eng. J.* 390, 124641.
- Wang, X., Wang, X., Shao, Y., Jin, B., 2020c. Three-dimensional modelling of the multiphase hydrodynamics in a separated-gasification chemical looping combustion unit during full-loop operation. *J. Clean. Prod.* 275, 122782.
- Wang, X., Shao, Y., Jin, B., 2021a. Spatiotemporal statistical characteristics of multiphase flow behaviors in fuel reactor for separated-gasification chemical looping combustion of solid fuel. *Chem. Eng. J.* 412, 128575.
- Wang, X., Shao, Y., Jin, B., 2021b. Thermodynamic evaluation and modelling of an auto-thermal hybrid system of chemical looping combustion and air separation for power generation coupling with CO₂ cycles. *Energy* 236, 121431.
- Wei, G., He, F., Huang, Z., Zheng, A., Zhao, K., Li, H., 2015. Continuous operation of a 10 kW_{th} chemical looping integrated fluidized bed reactor for gasifying biomass using an iron-based oxygen carrier. *ENERG FUEL* 29, 233–241.
- Wei, G., Zhao, W., Meng, J., Feng, J., Li, W., He, F., Huang, Z., Yi, Q., Du, Z., Zhao, K., Zhao, Z., Li, H., 2018. Hydrogen production from vegetable oil via a chemical looping process with hematite oxygen carriers. *J. Clean. Prod.* 200, 588–597.
- Weng, Q., Toan, S., Ai, R., Sun, Z., Sun, Z., 2021. Ammonia production from biomass via a chemical looping-based hybrid system. *J. Clean. Prod.* 289, 125749.
- Xue, N., Wang, Z., Wu, J., He, T., Zhang, J., Li, J., Wu, J., 2019. Effect of equivalence ratio on the CO selectivity of Fe/Ca-based oxygen carriers in biomass char chemical looping gasification. *Fuel* 252, 220–227.
- Yan, X., Hu, J., Zhang, Q., Zhao, S., Dang, J., Wang, W., 2020. Chemical-looping gasification of corn straw with Fe-based oxygen carrier: thermogravimetric analysis. *BIORESOURCE TECHNOL* 303, 122904.
- Yu, Z., Yang, Y., Yang, S., Zhang, Q., Zhao, J., Fang, Y., Hao, X., Guan, G., 2019. Iron-based oxygen carriers in chemical looping conversions: a review. *Carbon Resources Conversion* 2, 23–34.
- Zeng, J., Xiao, R., Zeng, D., Zhao, Y., Zhang, H., Shen, D., 2015. High H₂/CO ratio syngas production from chemical looping gasification of sawdust in a dual fluidized bed gasifier. *ENERG FUEL* 30, 1764–1770.
- Zheng, A., Fan, Y., Wei, G., Zhao, K., Huang, Z., Zhao, Z., Li, H., 2020. Chemical looping gasification of torrefied biomass using NiFe₂O₄ as an oxygen carrier for syngas production and tar removal. *ENERG FUEL* 34, 6008–6019.
- Zylka, A., Krzywanski, J., Czakiert, T., Idziak, K., Sosnowski, M., de Souza-Santos, M.L., Sztokler, K., Nowak, W., 2020. Modeling of the chemical looping combustion of hard coal and biomass using ilmenite as the oxygen carrier. *Energies* 13, 5394.
- Zylka, A., Krzywanski, J., Czakiert, T., Idziak, K., Sosnowski, M., Grabowska, K., Prauzner, T., Nowak, W., 2019. The 4th Generation of CeSFaMB in numerical simulations for CuO-based oxygen carrier in CLC system. *Fuel* 255, 115776.